Pakula, A. A., & Sauer, R. T. (1990) *Nature 344*, 363.
Pauling, L., & Corey, R. B. (1954) *Proc. Natl. Acad. Sci. U.S.A. 37*, 729.
Presta, L. G., & Rose, G. D. (1988) *Science 240*, 1632.
Privalov, P. L. (1979) *Adv. Protein Chem. 33*, 167.
Radzicka, A., & Wolfenden, R. (1988) *Biochemistry 27*, 1644.
Richards, F. M. (1977) *Annu. Rev. Biophys. Bioeng. 6*, 151.
Sandberg, W. S., & Terwilliger, T. C. (1991) *Proc. Natl. Acad. Sci. U.S.A. 88*, 1706.
Sato, K., & Egami, F. (1957) *J. Biochem. (Tokyo) 44*, 753.
Scholtz, J. M., Marqusee, S., Baldwin, R. L., York, E. J., Stewart, J. M., Santoro, M., & Bolen, D. W. (1991) *Proc. Natl. Acad. Sci. U.S.A. 88*, 2854.
Sharp, K. A., Nicholls, A., Fine, R. F., & Honig, B. (1991a) *Science 252*, 106.
Sharp, K. A., Nicholls, A., Friedman, R., & Honig, B. (1991b) *Biochemistry 30*, 9686.
Shirley, B. A., & Laurents, D. V. (1990) *J. Biochem. Biophys. Methods 20*, 181.
Shirley, B. A., Stanssens, P., Steyaert, J., & Pace, C. N. (1989) *J. Biol. Chem. 264*, 11621.
Shortle, D., Stites, W. E., & Meeker, A. K. (1990) *Biochemistry 29*, 8033.
Spolar, R. S., Ha, J. H., & Record, M. T. (1989) *Proc. Natl. Acad. Sci. U.S.A. 86*, 8382.
Stanssens, P., Opsomer, C., McKeown, Y. M., Kramer, W., Zabeau, M., & Fritz, H. J. (1989) *Nucleic Acids Res. 17*, 4441.
Steyaert, J., Opsomer, C., Wyns, L., & Stanssens, P. (1991) *Biochemistry 30*, 494.
Street, I. P., Armstrong, C. R., & Withers, S. G. (1986) *Biochemistry 25*, 6021.
Tanford, C. (1962) *J. Am. Chem. Soc. 84*, 4240.
Tanner, N. K., & Cech, T. R. (1987) *Biochemistry 26*, 3330.
Thomson, J. A., Shirley, B. A., Grimsley, G. R., & Pace, C. N. (1989) *J. Biol. Chem. 264*, 11614.
Yutani, K., Ogasahara, K., Tsujita, T., & Sugino, Y. (1987) *Proc. Natl. Acad. Sci. U.S.A. 84*, 4441.

Mechanism of the Conformational Transition of Melittin†

Yuji Goto* and Yoshihisa Hagihara
Department of Biology, Faculty of Science, Osaka University, Toyonaka, Osaka 560, Japan
Received July 15, 1991; Revised Manuscript Received October 17, 1991

ABSTRACT: It is known that, while melittin at micromolar concentrations is unfolded under conditions of low ionic strength at neutral pH, it adopts a tetrameric α-helical structure under conditions of high ionic strength, at alkaline pH, or at high peptide concentrations. To understand the mechanism of the conformational transition of melittin, we examined in detail the conformation of melittin under various conditions by far-UV circular dichroism at 20 °C. We found that the helical conformation is also stabilized by strong acids such as perchloric acid. The effects of various acids varied largely and were similar to those of the corresponding salts, indicating that the anions are responsible for the salt- or acid-induced transitions. The order of effectiveness of various monovalent anions was consistent with the electroselectivity series of anions toward anion-exchange resins, indicating that the anion binding is responsible for the salt- or acid-induced transitions. From the NaCl-, HCl-, and alkaline pH-induced conformational transitions, we constructed a phase diagram of the anion- and pH-dependent conformational transition. The phase diagram was similar in shape to that of acid-denatured apomyoglobin [Goto, Y., & Fink, A. L. (1990) *J. Mol. Biol. 214*, 803–805] or that of the amphiphilic Lys, Leu model polypeptide [Goto, Y., & Aimoto, S. (1991) *J. Mol. Biol. 218*, 387–396], suggesting a common mechanism of the conformational transition. The anion-, pH-, and peptide concentration-dependent conformational transition of melittin was explained on the basis of an equation in which the conformational transition is linked to proton and anion binding to the titratable groups.

The conformational stability of monomeric α-helical peptides has been useful for elucidating the factors stabilizing or destabilizing the α-helices of globular proteins (Marqusee & Baldwin, 1987; Shoemaker et al., 1987; Bradley et al., 1990; Lyu et al., 1990; Padmanabhan et al., 1990). To extend our understanding of protein folding, it is important to study peptides which form an oligomeric structure stabilized by long-range interactions, because such interactions are also important in determining the conformational stability of peptides and proteins (DeGrado & Lear, 1985; Kim & Baldwin, 1990).

Melittin, a bee venom toxin, is a suitable model for this purpose. Melittin consists of 26 amino acid residues, 5 of which are basic but none of which are acidic (Habermann, 1972). The conformational properties of melittin have been studied extensively in relation to the interaction of peptides with biological membranes (Talbot et al., 1979; Knoppel et al., 1979; Lauterwein et al., 1980; Brown et al., 1980; Bello et al., 1982; Quay & Condie, 1983; Inagaki et al., 1989). It has been shown that, whereas melittin assumes a monomeric helical structure in methanol or in membranes, its conformation in aqueous solution depends on ionic and pH conditions. Whereas melittin at micromolar concentrations is unfolded under conditions of low ionic strength at neutral pH, it adopts a tetrameric helical structure under conditions of high ionic strength or at alkaline pH. The X-ray structure of tetrameric melittin crystallized from aqueous solution has been reported (Terwilliger & Eisenberg, 1982a,b). Because the conformational transition accompanies a monomer-to-tetramer reaction, high peptide concentrations also favor the helical structure

† This work was supported in part by Grants-in-Aid for Scientific Research from the Ministry of Education, Science and Culture of Japan.
* Author to whom correspondence should be addressed.

0006-2960/92/0431-732$03.00/0

(Talbot et al., 1979; Brown et al., 1980; Bello et al., 1982; Quay & Condie, 1983). It is generally assumed that salt or alkaline pH reduces the electrostatic repulsion between the positive charges, resulting in formation of the helical structure. However, the exact mechanism and interrelationship of the conformational transitions are unknown.

A series of studies by Goto and A. L. Fink (Goto & Fink, 1989, 1990; Goto et al., 1990a,b) showed that the conformation of acid-denatured proteins depends on ionic conditions. While acid-denatured proteins including cytochrome *c*, β-lactamase, and apomyoglobin are largely unfolded at around pH 2 under conditions of low ionic strength, addition of anions from either salt or acid induces the refolding transition to a molten globule, a compact structure with a significant amount of secondary structure but a disordered tertiary structure (Ohgushi & Wada, 1983; Ptitsyn, 1987; Kuwajima, 1989).

To study the role of the anion-dependent conformational transition at neutral pH, Goto and Aimoto (1991) prepared an amphiphilic model peptide of 51 amino acid residues, consisting of tandem repeats of a Lys-Lys-Leu-Leu sequence and containing a turn sequence, Asn-Pro-Gly, at the center of the molecule. Whereas the model polypeptide showed no significant conformation under conditions of low salt at neutral pH, addition of anions, either from salt or from acid, induced the folding transition to a monomeric α-helical state, in which two amphiphilic helices interact with each other intramolecularly through hydrophobic Leu residues. The results show that the anion binding-dependent conformational transition is not limited to the acid-denatured proteins but could also occur to the positively charged amphiphilic polypeptide at neutral pH.

The conformation of acid-denatured proteins or the model polypeptide is determined by a balance of repulsive forces, which favor the extended unfolded state, and the opposing forces, mainly hydrophobic interactions, which favor the folded state. The binding of anions to the positive charges shields the repulsive forces, allowing the intrinsic hydrophobic forces to manifest themselves.

These results suggested that this mechanism is of general importance for the conformational stability of proteins and peptides. Since melittin is a basic peptide showing salt- and pH-dependent conformational transitions, it is an excellent model for examining this concept. We show here that the anion-, pH-, and peptide concentration-dependent conformational transition of melittin is very similar to that of the acid-denatured proteins or the Lys, Leu model polypeptide and can be explained simply on the basis of an equation in which the conformational transition is linked to proton and anion binding to the titratable groups.

Materials and Methods

Materials. A crude melittin, purchased from Sigma, was applied to a preparative C_{18} high-pressure liquid chromatography column, and the major sharp peak, eluted with a gradient of acetonitrile in 0.05% trifluoroacetic acid, was collected and stored after lyophilization. Other chemicals were of reagent grade and were used without further purification.

Methods. Circular dichroism (CD)[1] measurements were carried out with a Jasco spectropolarimeter, Model J-500A, equipped with an interface and a personal computer. The instrument was calibrated with ammonium *d*-10-camphorsulfoic acid. The results are expressed as the mean residue ellipticity, $[\theta]$, which is defined as $[\theta] = 100\theta_{obsd}/lc$, where θ_{obsd} is the observed ellipticity in degrees, c is the concentration in residue moles per liter, and l is the length of the light path in centimeters. The measurements were carried out at 20 °C with thermostatically controlled cell holders.

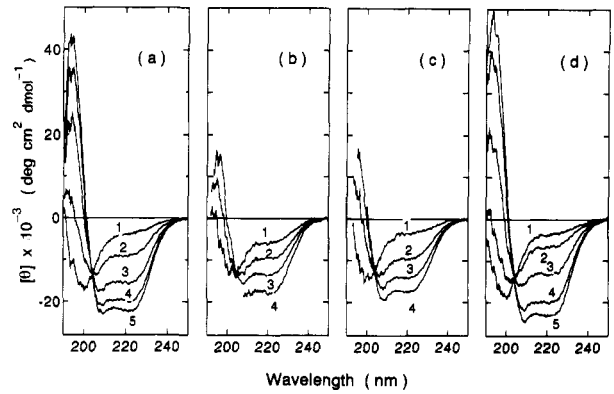

FIGURE 1: Far-UV CD spectra of melittin as a function of $NaClO_4$ concentration in 10 mM Tris-HCl buffer (pH 7.5) (a), of alkaline pH (b), of melittin concentration in 10 mM sodium acetate buffer at pH 4.7 (c), and of $HClO_4$ concentration (d). (Panel a) $NaClO_4$ concentration: 1, 0 mM; 2, 53 mM; 3, 88 mM; 4, 176 mM; 5, 440 mM. (Panel b) Buffer and pH: 1, 10 mM Tris-HCl (pH 7.5); 2, 10 mM CHES buffer (pH 9.5); 3, 5 mM NaOH (pH 11.3); 4, 88 mM NaOH (pH 12.6). (Panel c) Melittin concentration: 1, 0.5 mM; 2, 4.3 mM; 3, 6.1 mM; 4, 8.2 mM. (Panel d) $HClO_4$ concentration and pH: 1, 0 mM (pH 5); 2, 44 mM (pH 1.5); 3, 88 mM (pH 1.1); 4, 176 mM (pH 0.8); 5, 440 mM (pH 0.5).

Usually, 0.1 mL of melittin solution, dissolved in deionized water, was mixed with 0.9 mL of salt, acid, or alkaline solutions. The CD spectra were measured, unless otherwise specified, at a peptide concentration of 27.6 μM with a 1-mm cell. For the measurements at high melittin concentration, cells of 0.1- and 0.02-mm path length were used. The peptide concentration was determined from the absorption at 280 nm using a molar absorption coefficient of 5570 (Quay & Condie, 1983). The pH was measured soon after spectroscopic measurement, using a Radiometer PHM83 at 20 °C.

Results

Conformational Transitions of Melittin. Figure 1 shows the far-UV CD spectra of melittin under various conditions at 20 °C. In the absence of salt at pH 2–8, the CD spectrum of melittin (27.6 μM) showed a minimum at 200 nm, indicating the absence of any significant secondary structure in the polypeptide.

As described above, it has been shown that melittin can be transformed to an α-helical conformation in three different ways. First, as shown in Figure 1a, the addition of salt [sodium perchlorate ($NaClO_4$) in this case] changed the spectrum of the unfolded conformation to one showing minima at 208 and 222 nm, representing the formation of α-helix. The spectra at different concentrations of $NaClO_4$ showed an isodichroic point at 204 nm, consistent with a two-state transition. Second, the increase in pH induced the α-helical conformation (Figure 1b). Third, the increase in peptide concentration also produced the helical conformation (Figure 1c).

In addition to these conditions, we found that the helical conformation is also stabilized by strong acids such as perchloric acid ($HClO_4$) (Figure 1d). This finding was based on a suggestion obtained from acid-denatured proteins or the model polypeptide, in which the effects of strong acids were similar to those of corresponding salts. As can be seen from Figure 1, the CD spectra of the helical states were similar, indicating that the helical conformation is relatively constant

[1] Abbreviations: CAPS, 3-(cyclohexylamino)-1-propanesulfonic acid; CD, circular dichroism; CHES, 2-(*N*-cyclohexylamino)ethanesulfonic acid; NMR, nuclear magnetic resonance.

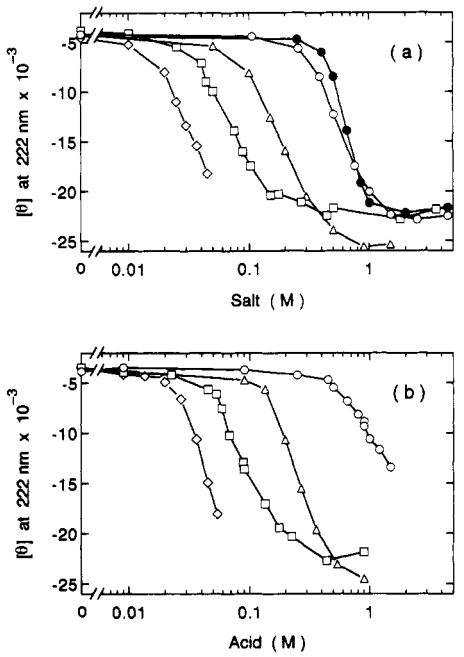

FIGURE 2: Folding transitions of melittin induced by various monovalent salts in 10 mM Tris-HCl buffer (pH 7.5) (a) or by monovalent acids without a buffer component (b) at 20 °C measured by the change in ellipticity at 222 nm. Salts used were KF (●), NaCl (○), sodium trifluoroacetate (△), $NaClO_4$ (□), and sodium trichloroacetate (◇). Acids were HCl (○), trifluoroacetic acid (△), $HClO_4$ (□), and trichloroacetic acid (◇).

independent of the conditions stabilizing it.

(1) Salt- and Acid-Induced Transitions. To elucidate the mechanism by which these different conditions stabilize similar helical conformations, we first compared the effects of various salts (Figure 2a). Although the values of maximal ellipticity differed slightly depending on the salt species, all of the monovalent salts examined induced similar α-helical conformations. However, the salt concentration range required to bring about the transition varied greatly among the different salts. In the case of sodium trichloroacetate, the later stage of the transition could not be measured due to high absorption of the solvents. The salts used were those of sodium or potassium. Because the transition induced by KCl (not shown) was similar to that induced by NaCl, the large difference in the effects of various salts was due to differences in the effects of the anions.

Figure 2b compares the effects of various acids in stabilizing the helical state. The order of effectiveness is consistent with that of salts, and the concentration range of acids required to bring about the transition is similar to that of the corresponding salts except for HCl, which required a higher concentration than NaCl. These results support the idea that the anion is important. The order of effectiveness of anions is

$$\text{trichloroacetate} > ClO_4^- > \text{trifluoroacetate} > Cl^- > F^- \quad (1)$$

This series is consistent with the order of effectiveness of anions for stabilizing the molten globule state of acid-denatured proteins (Goto et al., 1990b) or the corresponding state of the Lys, Leu model polypeptide (Goto & Aimoto, 1991), and also with the electroselectivity series of anions toward anion-exchange resins (Gregor et al., 1955; Gjerde et al., 1980). The electroselectivity series represents the order of affinity of anions toward the positive charges on the resins. This indicates that the anion binding is responsible for the salt- or acid-induced conformational transition of melittin. It should be noted that the order of the series in eq 1 is opposite of that of the monovalent anions stabilizing the native structure of proteins [i.e., the Hofmeister series; see von Hippel and Schleich (1969) and Collins and Washabaugh (1985)]. Chaotropic anions, which are located to the left of chloride and have a higher tendency to denature the native proteins, showed a higher tendency to stabilize the helical state of melittin.

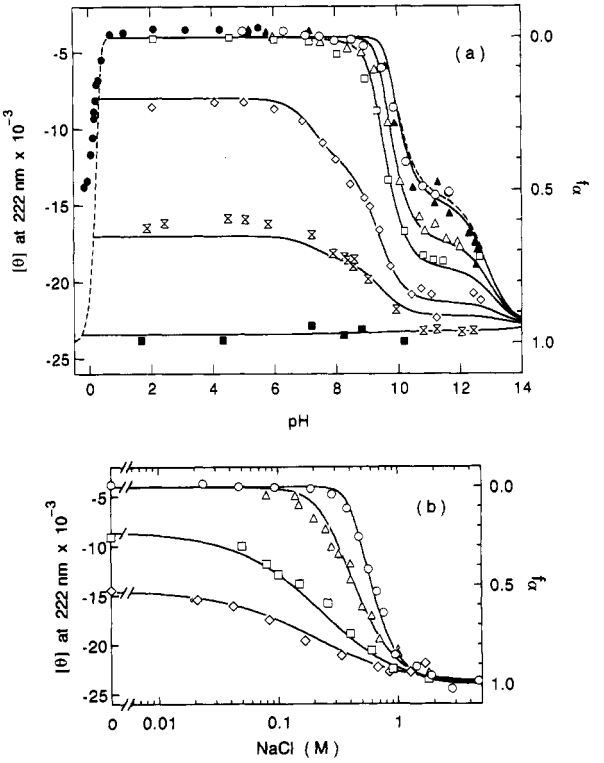

FIGURE 3: Dependence of the ellipticity of melittin at 222 nm on the pH (a) at different ionic strengths and on NaCl concentration (b) at different pHs, at 20 °C. The values of ionic strength in panel a were 0.01 (○), 0.09 (△), 0.18 (□), 0.45 (◇), 0.71 (⧖), and 1.77 (■), where the ionic strength of the buffer component was less than 0.01 and the total ionic strength was controlled by NaCl. The buffers used were sodium acetate (pH 3–6.5), Tris-HCl (pH 6.5–8.5), CHES (pH 8.5–9.5), and CAPS (pH 9.5–11). The solutions below pH 3 were prepared using the appropriate concentration of HCl. Solid circles and solid triangles represent the HCl-induced transition taken from Figure 2 and the NaOH-induced transition, respectively, where the ionic strength is minimal at each pH. The pH values in panel b were 4.7 (○), 8.9 (△), 10.0 (□), and 11.4 (◇). The ionic strength of the buffer component was less than 0.01. The right-hand scale indicates the fraction of melittin folded (f_α). The lines were calculated using eq 5 and the parameters in Table I.

We also examined the effects of salts involving multivalent anions. The multivalent anions generally showed a marked tendency to precipitate the protein, suggesting that the tight interactions of melittin with multivalent anions are not compatible with the helical conformation. Although the results obtained were not complete, the general trend was consistent with the electroselectivity series (data not shown).

(2) Alkaline pH-Induced Transition. Figure 3a shows the alkaline pH-induced transition under different conditions of ionic strength measured by the change in ellipticity at 222 nm. At low ionic strength, the alkaline pH-induced transition, which started at pH 9, was a two-step one with a shoulder at around pH 11. As the ionic strength increased, under control with NaCl, the three-step nature of the transition became evident, although the amplitude of the ellipticity change became small. At an ionic strength of 0.45, the conformational transition, which started at pH 6.5, had shoulders at pH 8.5 and 11. A similar stepwise alkaline transition has also been reported by Bello et al. (1982). Since melittin has one α-

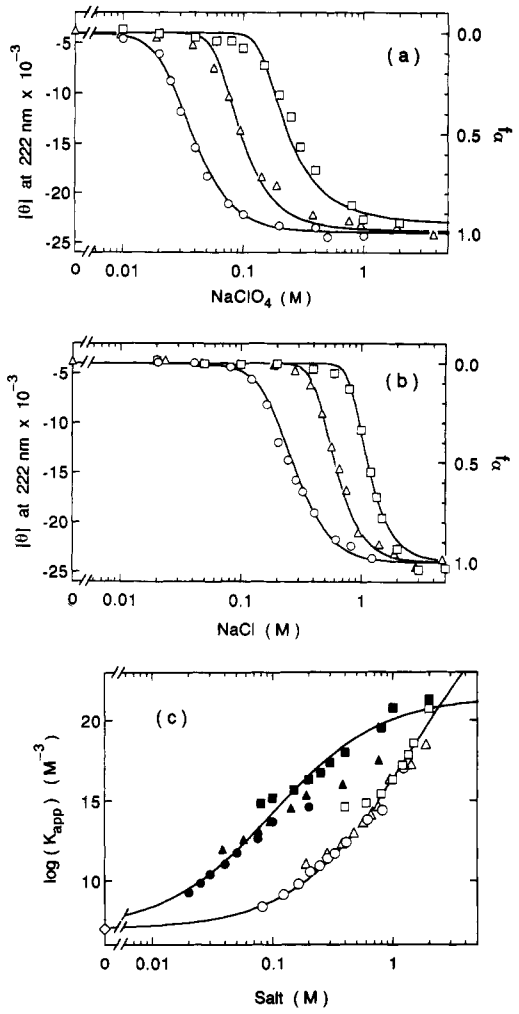

FIGURE 4: Dependence on peptide concentration of the $NaClO_4$-induced (a) and NaCl-induced (b) folding transitions measured by the change in ellipticity at 222 nm in 10 mM sodium acetate buffer (pH 4.7) at 20 °C. Peptide concentrations in (a) were 2.6 (□), 25.9 (△), and 259 μM (○). Those in (b) were 2.8 (□), 27.6 (△), and 276 μM (○). Cells with 0.1-, 1-, and 10-mm path lengths were used for the high, medium, and low peptide concentrations, respectively. The right-hand scale in panels a and b indicates the fraction of melittin folded (f_α). Panel c shows the dependence of K_{app} on salt concentration obtained on the basis of eq 2. Open symbols are for the NaCl-induced transition, and solid symbols are for the $NaClO_4$-induced transition. The diamond indicates the K_{app} in the absence of salt in 10 mM sodium acetate buffer (pH 4.7). The value indicates the average of five points obtained from the peptide concentration-dependent conformational transition as shown in Figure 1c. The lines for NaCl-dependent transitions were calculated using eq 5, $K_f^{UH6} = 1.0 \times 10^7$, and the parameters in Table I. The lines for $NaClO_4$-dependent transitions were calculated using eq 5, $K_f^{UH6} = 1.0 \times 10^7$, and the parameters in Table I, except K_A^{UH} and K_A^{FH} were assumed to be 5 and 20, respectively, for all the titratable groups.

amino, three ε-amino (Lys-7, Lys-21, and Lys-23), and two guanidyl (Arg-22 and Arg-24) groups as titratable groups, the stepwise transition was suggested to be related to the deprotonation of these groups.

Figure 3b shows the NaCl-induced transitions at different pH values. Because the helical state is stabilized at alkaline pH, the amplitude of the ellipticity change decreased with the increase in pH.

(3) Dependence of the Transition on Peptide Concentration. Because the helical state of melittin is tetrameric, the salt-induced transition is dependent on the peptide concentration. Panels a and b of Figure 4 show the $NaClO_4$- and NaCl-induced transitions, respectively, at different peptide concentrations. The conformational transition shifted to lower salt concentrations with an increase in the peptide concentration. The transition was analyzed assuming a monomer-to-tetramer mechanism, in which the monomer is unfolded (U) and the tetramer folded (F_4)

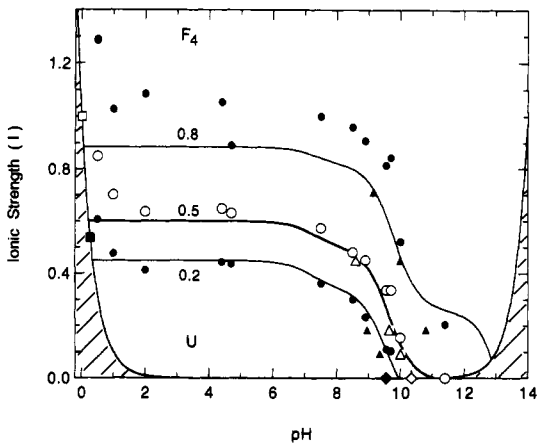

FIGURE 5: Phase diagram for the unfolded (U) and folded (F_4) helical states of melittin at 27.6 μM at 20 °C. The 20% (closed), 50% (open), and 80% (closed) stages of the folding transition were estimated from the NaCl-induced transitions at various pH values (●, ○), the pH-induced transitions at various ionic strengths (▲, △), the HCl-induced transition (■, □), and the NaOH-induced transition (♦, ◇). The ionic strength of the buffer component was less than 0.01, and the total ionic strength was controlled by [NaCl]. The hatched area is prohibited due to the increase in the minimum ionic strength with a decrease or increase in pH. The contour lines corresponding to 20%, 50%, and 80% stages of the folding transition were calculated on the basis of eq 5 and the parameters in Table I.

mechanism 1

$$4U \rightleftharpoons F_4$$

The apparent equilibrium constant (K_{app}) for the folding transition was obtained from the ellipticity at 222 nm by

$$K_{app} = \frac{[F_4]}{[U]^4} = \frac{[\theta]_U - [\theta]}{4([\theta] - [\theta]_F)^4} \quad (2)$$

where $[\theta]_U$ and $[\theta]_F$ are the ellipticities for the unfolded and folded states, respectively, and $[\theta]$ is the observed ellipticity. As shown in Figure 4c, the values of K_{app} obtained at different peptide concentrations agreed well, being consistent with mechanism 1.

Figure 4c also shows the value of K_{app} in the absence of salt at pH 4.7, which was estimated from the conformational transition induced with the increase in melittin concentration (Figure 1c). The K_{app} value (1.0×10^7 M^{-3}) in the absence of salt was on the extrapolation of the values obtained in the presence of salt.

Phase Diagram of the Conformational States. Although the helical state is tetrameric, the conformational transitions of melittin are very similar to those of acid-denatured proteins (Goto & Fink, 1989, 1990; Goto et al., 1990a,b) or the Lys, Leu model polypeptide (Goto & Aimoto, 1991). The similarity can be further represented by a phase diagram of the helical (F_4) and unfolded (U) states.

From the NaCl-, HCl-, and alkaline pH-induced conformational transitions at a peptide concentration of 27.6 μM, we constructed a phase diagram of melittin (Figure 5) based on assumptions that the transition is a two-state one (mechanism 1) and that the helical states are the same. The left- and right-hand boundaries of the phase diagram correspond to the ionic strength of HCl ($I = 10^{-pH}$) or NaOH alone ($I = 10^{pH-14}$) at the given pH, and the hatched area is prohibited because of the increase in the minimal ionic strength with the decrease or increase in pH. The unfolded state is stable below

pH 9 under conditions of low ionic strength ($I < 0.4$). It is seen that the HCl-induced conformational transition can be explained by an increase in the minimum concentration of anion with a decrease in pH, although HCl required a higher concentration than NaCl to induce the transition. The phase diagram is similar in shape to that of acid-denatured apomyoglobin [Figure 2 of Goto and Fink (1990)] or the model polypeptide [Figure 7 of Goto and Aimoto (1991)], suggesting a common mechanism of conformational transition.

Discussion

We have shown the folding transitions of melittin produced under various conditions. The results indicate that the conformation of melittin is determined by a balance of the charge repulsions between positive groups and the opposing forces stabilizing the helical state and that anion binding and deprotonation of titratable groups modulate the balance. Although there have been many studies on the conformation of melittin and, as a result, the stabilization of the helical state by salts is well-known, the exact mechanism of the salt effects has been unknown. Our results clearly show that anion binding is responsible for it. On the basis of the finding that anion binding stabilizes the helical state, we consider the mechanism of the conformational transition of melittin.

Mechanism of the Conformational Transition. To consider the mechanism, it should be emphasized that the conformational transition of melittin is similar to that of acid-denatured proteins (Goto & Fink, 1989, 1990) or the Lys, Leu model polypeptide (Goto & Aimoto, 1991). In particular, the anion- and pH-dependent conformational transition of the Lys, Leu model polypeptide is basically the same as that of melittin. Goto and Aimoto (1991) explained the conformational transition of the Lys, Leu model polypeptide on the basis of a mechanism in which proton binding and anion binding are linked to the conformational transition and anions bind only to the protonated groups. We assumed that the mechanism is also applicable to the case of melittin. A monomeric transition between the unfolded (U) and folded (F) states with one titratable group is represented by mechanism 2 where

mechanism 2

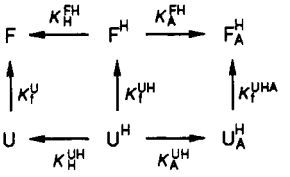

species with the superscript H represent the protonated species and those with the subscript A represent the species with bound anion. K_f^{UH}, K_A^{UH}, K_A^{FH}, etc. represent the equilibrium constants of the respective processes indicated by arrows. The K_{app} for the folding transition is expressed as

$$K_{app} = \frac{[F] + [F^H] + [F_A^H]}{[U] + [U^H] + [U_A^H]} = K_f^{UH}\frac{1 + K_A^{FH}[A] + K_H^{FH}/[H]}{1 + K_A^{UH}[A] + K_H^{UH}/[H]} \quad (3)$$

The K_{app} for the monomeric transition with n titratable groups, assuming independence of the groups, is represented as

$$K_{app} = K_f^{UHn}\prod_{i=1}^{n}\frac{1 + K_{Ai}^{FH}[A] + K_{Hi}^{FH}/[H]}{1 + K_{Ai}^{UH}[A] + K_{Hi}^{UH}/[H]} \quad (4)$$

where K_f^{UHn} is the equilibrium constant for the fully protonated species, and the subscript i indicates that the constant is for the ith group. Equation 4 can be further extended for the conformational transition between the monomeric unfolded and oligomeric folded states, provided that we assume independence of the groups both in and between the subunits. In the case of the monomer-to-tetramer transition of melittin with six titratable groups, K_{app} is represented by

$$K_{app} = K_f^{UH6}\prod_{i=1}^{6}\frac{(1 + K_{Ai}^{FH}[A] + K_{Hi}^{FH}/[H])^4}{(1 + K_{Ai}^{UH}[A] + K_{Hi}^{UH}/[H])^4} \quad (5)$$

where K_f^{UH6} is the equilibrium constant of the monomer-to-tetramer transition for the six-protonated species.

Table I: Conformational Parameters of Melittin Obtained on the Basis of eq 5 and $K_f^{UH6} = 1.0 \times 10^7$ at 20 °C[a]

	pK_H^{UH}	pK_H^{FH}	K_A^{UH} (M^{-1})	K_A^{FH} (M^{-1})
α-amino	7.35	6.9	0.2	2
three lysyl amino	9.69	9.25	0.15	1.5
two guanidyl	13.5	13.0	0.4	3.1

[a] The values of the same groups were assumed to the same. pK_H^{UH} is $-\log K_H^{UH}$, and pK_H^{FH} is $-\log K_H^{FH}$.

Because the shoulders in the pH-induced folding transition (Figure 3a) suggested the contributions of several titratable groups, we used eq 5, which takes into account all the titratable groups, to analyze the conformational transitions. The value of K_f^{UH6} was assumed to be equal to the value of K_{app} (1.0×10^7 M^{-3}) in 10 mM acetate buffer at pH 4.7. As a first approximation, it was considered that groups of the same kind (three ϵ-amino and two guanidyl groups) are indistinguishable. Then, the 12 parameters of eq 5 were determined so that the calculated curves fitted all the experimental data: i.e., the pH-dependent transitions at various NaCl concentrations (Figure 3a) and NaCl-dependent transitions at various pH values (Figure 3b) and various peptide concentrations (Figure 4a). The fitting was carried out manually. Although there are many adjustable parameters, the folding transitions obtained under various conditions defined a unique set of parameters (Table I). As shown in Figures 3–5, the conformational transitions were simulated satisfactorily by eq 5 and a single set of parameters.

Importance of Counterion Binding. As described above, the folding transitions of melittin produced under various conditions are explained by eq 5, which is based on the linkage of the conformational transition with anion binding and also with deprotonation of independent titratable groups. Although we neglected the contributions of other factors such as Debye–Hückel screening effects of ions (see below), at the present stage of research, it is important to note that such a simple mechanism largely explains the complicated conformational transitions of melittin. Because the conformational transitions of the acidic molten globule state (Goto et al., 1990b; Goto & Fink, 1990) and the corresponding state of the Lys, Leu model polypeptide (Goto & Aimoto, 1991) were also explained in a similar way, this mechanism may be of critical importance when the net charge is high and the stability of a folded state is marginal.

Recently, Stigter et al. (1991) have reported the electrostatic stability of globular proteins on the basis of a theoretical model that takes into account the hydrophobic interaction, chain conformational entropy, and electrostatic effects. In their smeared-charge Poisson–Boltzmann theory of the electrostatics of folded and unfolded states, salts were assumed to affect the electrostatic interactions of proteins by modulating the dielectric constant of outside and porous inside of the protein conformational states. Salt effects were treated in terms of

ionic strength. They have predicted the salt-dependent two populations of denatured species, one open and the other more compact, with densities in the range found experimentally for molten globule states. In addition, they have predicted a phase diagram (stability vs pH, ionic strength) for the different conformational states. Their results are surprisingly in good agreement with the experiments of Goto and Fink (1989, 1990) on β-lactamase and apomyoglobin obtained with chloride as an anion. It would be possible to predict the conformational transition of melittin on the basis of the same theoretical model.

However, because the salt effects were considered by ionic strength, their theory explains none of the large differences in the effects of various monovalent anions as observed for melittin (Figure 2a), the acid-denatured proteins (Goto et al., 1990a,b), and the Lys, Leu model polypeptide (Goto & Aimoto, 1991). For example, whereas melittin at 27.6 μM takes the helical conformation in 0.1 M sodium perchlorate at pH 7.5, it is largely unfolded in 0.1 M sodium chloride at pH 7 even though the ionic strength is the same (Figure 2a). The large difference in the effects of various anions can be explained by the difference in the electroselectivity of anions toward positive groups of proteins and peptides. Thus, although the dielectric constant of the solution, which depends on the ionic strength, is of course an important factor determining the electrostatic interactions of charged groups on proteins and peptides (Matthew, 1985; Dill, 1990), the specific anion binding, which critically depends on ion species, is more important in determining the electrostatics of the acid-denatured proteins and positively charged peptides such as melittin.

Other Factors. The estimated pK_a values of the titratable groups in the unfolded state of melittin are smaller than the intrinsic pK_a values without electrostatic interactions (Tanford, 1968) (i.e., 7.8 for α-amino, 10.4 for lysyl amino, and >12.5 for guanidyl). The difference between the intrinsic and the estimated pK_a values for unfolded melittin reflects the electrostatic interactions between the condensed positive groups on the monomeric melittin molecule, since such interactions would be expected to decrease the pK_a values. The pK_a values decreased further upon formation of the compact folded state. In a similar way, the constants (K_A^{UH}, K_A^{FH}) of binding of chloride ions to the protonated groups, which is intrinsically low in the unfolded state, were increased 10-fold upon formation of the folded state. Thus, although we assumed independence of the titratable groups, in which the electrostatic interactions between the titratable groups were included in the change in the intrinsic pK_a value or the intrinsic binding constant for anions, the importance of the electrostatic interactions between titratable groups is evident, and the exact mechanism should be more complicated than our approximation.

Lauterwein et al. (1980), on the basis of a ^{1}H NMR study, reported a pK_a value of 7.7 for the α-amino group of monomeric melittin, which is slightly larger than the value (7.35) we estimated. Although Bello et al. (1982) estimated apparent pK_a values of 7.2 and 9.6 at a peptide concentration of 80 μM in 0.02 M sodium phosphate buffer from the alkali-induced transition measured by CD, the apparent values cannot be compared with our values because, as expected from eq 5, it is a complicated function of the pK_a values of the folded and unfolded states, the value of K_f^{UH6}, and the peptide concentration. Quay and Tronson (1983) estimated the pK_a values of Lys-21 and Lys-23 of monomeric melittin to be 6.5 and 8.6, respectively, from the reactivity of amino groups toward 2,4,6-trinitrobenzenesulfonate. However, because the modifying reagent has a negative charge, it is possible that the reaction was affected by electrostatic interactions between the reagent and the positive groups of melittin. The validation of the pK_a values in Table I awaits further study, although, as a first approximation, they account for most of the observed conformational transitions. To understand the exact mechanism, it will also be necessary to estimate the contributions of other factors such as Debye–Hückel screening effects, which are reflected in a change in the effective dielectric constant as described above.

Finally, although chaotropic anions stabilize the folded state of melittin, this does not mean that the driving force of melittin folding is different from those of globular proteins. Whereas chaotropic anions, generally at high concentrations, denature the native protein structure by weakening the folding forces (i.e., hydrophobic interactions of proteins) through their effects on water, chaotropic anions, at relatively low concentrations, stabilize the helical structure of melittin by weakening the unfolding forces (i.e., charge repulsions) through direct and relatively nonspecific interactions with the positive groups of melittin. In both cases, however, the major driving forces of folding would be the hydrophobic interactions and van der Waals interactions due to close packing in the folded state. The present results emphasize that not only the effects on water and the Debye–Hückel screening effects but also direct interaction with positive groups on proteins is an important mechanism whereby anions affect the electrostatic stability of proteins and peptides.

ACKNOWLEDGMENTS

We thank Profs. K. Hamaguchi and S. Aimoto, Osaka University, for stimulating discussions and N. Okamura for assistance with the experiments.

Registry No. Melittin, 20449-79-0.

REFERENCES

Bello, J., Bello, H. R., & Granados, E. (1982) *Biochemistry 21*, 461–465.

Bradley, E. K., Thomason, J. F., Cohen, F. E., Kosen, P. A., & Kuntz, I. D. (1990) *J. Mol. Biol. 215*, 607–622.

Brown, L. R., Lauterwein, J., & Wüthrich, K. (1980) *Biochim. Biophys. Acta 622*, 231–244.

Collins, K. D., & Washabaugh, M. W. (1985) *Q. Rev. Biophys. 18*, 323–422.

DeGrado, W. F., & Lear, J. D. (1985) *J. Am. Chem. Soc. 107*, 7684–7689.

Dill, K. A. (1990) *Biochemistry 29*, 7133–7155.

Djerde, D. T., Schmuchler, G., & Fritz, J. S. (1980) *J. Chromatogr. 187*, 35–45.

Goto, Y., & Fink, A. L. (1989) *Biochemistry 28*, 945–952.

Goto, Y., & Fink, A. L. (1990) *J. Mol. Biol. 214*, 803–805.

Goto, Y., & Aimoto, S. (1991) *J. Mol. Biol. 218*, 387–396.

Goto, Y., Calciano, L. J., & Fink, A. L. (1990a) *Proc. Natl. Acad. Sci. U.S.A. 87*, 573–577.

Goto, Y., Takahashi, N., & Fink, A. L. (1990b) *Biochemistry 29*, 3480–3488.

Gregor, H. P., Belle, J., & Marcus, R. A. (1955) *J. Am. Chem. Soc. 77*, 2713–2719.

Habermann, H. (1972) *Science 177*, 314–322.

Inagaki, F., Shimada, I., Kawaguchi, K., Hirano, M., Terasawa, I., Ikura, T., & Go, N. (1989) *Biochemistry 28*, 5985–5991.

Kim, P. S., & Baldwin, R. L. (1990) *Annu. Rev. Biochem. 59*, 631–660.

Knoppel, E., Eisenberg, D., & Wickner, W. (1979) *Biochemistry 18*, 4177–4181.

Kuwajima, K. (1989) *Proteins: Struct., Funct., Genet. 6*, 87-103.
Lauterwein, J., Brown, L. R., & Wüthrich, K. (1980) *Biochim. Biophys. Acta 622*, 219-230.
Lyu, P. C., Life, M. I., Marky, L. A., & Kallenbach, N. R. (1990) *Science 250*, 669-673.
Marqusee, S., & Baldwin, R. L. (1987) *Proc. Natl. Acad. Sci. U.S.A. 84*, 8898-8902.
Matthew, J. B. (1985) *Annu. Rev. Biophys. Biophys. Chem. 14*, 387-417.
Ohgushi, M., & Wada, A. (1983) *FEBS Lett. 164*, 21-24.
Padmanabhan, S., Marqusee, S., Ridgeway, T., Laue, T. M., & Baldwin, R. L. (1990) *Nature 344*, 268-270.
Ptitsyn, O. B. (1987) *J. Protein Chem. 6*, 273-293.
Quay, S. C., & Condie, C. C. (1983) *Biochemistry 22*, 695-700.
Quay, S. C., & Tronson, L. P. (1983) *Biochemistry 22*, 700-707.
Shoemaker, K. R., Kim, P. S., York, E. J., Stewart, J. M., & Baldwin, R. L. (1987) *Nature 326*, 563-567.
Stigter, D., Alonso, D. O., & Dill, K. A. (1991) *Proc. Natl. Acad. Sci. U.S.A. 88*, 4176-4180.
Talbot, J. C., Dufourcq, J., deBony, J., Faucon, J. F., & Lussan, C. (1979) *FEBS Lett. 102*, 191-193.
Tanford, C. (1968) *Adv. Protein. Chem. 23*, 121-283.
Terwilliger, T. C., & Eisenberg, D. (1982a) *J. Biol. Chem. 257*, 6010-6015.
Terwilliger, T. C., & Eisenberg, D. (1982b) *J. Biol. Chem. 257*, 6016-6022.
von Hippel, P. H., & Schleich, T. (1969) in *Biological Macromolecules* (Timasheff, S., & Fasman, G., Eds.) Vol. II, pp 417-574, Marcel Dekker, New York.

Mechanism of Inhibition of Microtubule Polymerization by Colchicine: Inhibitory Potencies of Unliganded Colchicine and Tubulin–Colchicine Complexes†

Dimitrios A. Skoufias‡ and Leslie Wilson*
Department of Biological Sciences, University of California, Santa Barbara, California 93106
Received August 6, 1991; Revised Manuscript Received October 14, 1991

ABSTRACT: The tubulin–colchicine binding reaction appears to involve a number of intermediate steps beginning with rapid formation of a transient preequilibrium complex that is followed by one or more slow steps in which conformational changes in tubulin and colchicine lead to formation of a poorly reversible final-state complex. In the present study, we investigated the relative ability of unliganded colchicine and preformed final-stage tubulin–colchicine complex to incorporate at microtubule ends and to inhibit addition of tubulin at the net assembly ends of bovine brain microtubules in vitro. Addition of 0.1 μM final-stage tubulin–colchicine complex to suspensions of microtubules at polymer-mass steady-state resulted in rapid incorporation of one to two molecules of tubulin–colchicine complex per microtubule net assembly end concomitant with approximately 50–60% inhibition of tubulin addition. Incorporation of colchicine–tubulin complex continued slowly with time, without significant additional change in the rate of tubulin addition. In contrast, addition of unliganded colchicine to microtubule suspensions resulted in incorporation of small numbers of colchicine molecules at microtubule ends and inhibition of tubulin addition only after periods of time that varied from several minutes to approximately 20 min depending upon the concentration of colchicine. Inhibition of tubulin addition beginning with unliganded colchicine increased slowly with time, concomitant with increases in the concentration of final-state tubulin–colchicine complex and the amount of colchicine bound per microtubule end. The results indicate that inhibition of tubulin incorporation at microtubule ends is caused by colchicine-liganded tubulin in the form of a final-state complex. Unliganded colchicine and the transient preequilibrium complex either do not bind at all to microtubule ends or bind substantially more weakly than final-state TC complex.

Colchicine binds to tubulin and disrupts a diverse array of cellular processes by acting on the polymerization dynamics of microtubules [reviewed by Dustin (1984)]. It is clear that colchicine perturbs the exchange of tubulin at microtubule ends (Olmsted & Borisy, 1973; Margolis & Wilson, 1977; Sternlicht & Ringel, 1979; Margolis et al., 1980; Farrell & Wilson, 1980, 1984; Deery & Weisenberg, 1981; Bergen & Borisy, 1983, 1986; Lambeirs & Engleborghs, 1981; Andreu et al., 1983; Wilson et al., 1985; Wilson & Farrell, 1986; Medrano et al., 1989). However, a number of interesting aspects of the mechanism remain unresolved.

Extensive studies on the kinetics of colchicine binding to tubulin have indicated that the binding reaction occurs as a two-step process, with initial rapid formation of a transient, reversible, low-affinity preequilibrium complex followed by one or more slow steps in which conformational changes in the tubulin and in colchicine lead to formation of a very poorly reversible final-state tubulin–colchicine (TC)[1] complex [e.g.,

† Supported by USPHS Grant NS13560 from the National Institute of Neurological and Communicative Disorders and Stroke.
‡ Present address: Department of Zoology, University of California, Davis, CA 95616.

[1] Abbreviations: EGTA, ethylene glycol bis(β-aminoethyl ether)-*N,N,N',N'*-tetraacetic acid; GTP, guanosine 5'-triphosphate; GXP, guanine nucleotide in microtubules; MAP(s), microtubule-associated protein(s); MES, 2-(*N*-morpholino)ethanesulfonic acid; TC, tubulin–colchicine.

0006-2960/92/0431-738$03.00/0